

## VARIABILITY OF EGRET GAMMA-RAY SOURCES

P. L. NOLAN

W. W. Hansen Laboratory, Stanford University, Stanford CA 94305-4085, USA

W. F. TOMPKINS

Geophysical Associates, 324 Franklin St., Harrisonburg VA 22801, USA

I. A. GRENIER

Service d'Astrophysique, Centre d'Études de Saclay, 91991 Gif/Yvette, France

P. F. MICHELSON

Physics Department and W. W. Hansen Laboratory,  
Stanford University, Stanford CA 94305-4060, USA

Accepted by ApJ July 9, 2003

### ABSTRACT

The variability of the high-energy gamma ray sources in the Third *EGRET* catalog is analyzed by a new method. We re-analyze the *EGRET* data to calculate a likelihood function for the flux of each source in each observation, both for detections and upper limits. These functions can be combined in a uniform manner with a simple model of the flux distribution to characterize the flux variation by a confidence interval for the relative standard deviation of the flux. The main result is a table of these values for almost all the cataloged sources. As expected, the identified pulsars are steady emitters and the blazars are mostly highly variable. The unidentified sources are heterogeneous, with greater variation at higher Galactic latitude. There is an indication that pulsar wind nebulae are associated with variable sources. There is a population of variable sources along the Galactic plane, concentrated in the inner spiral arms.

*Subject headings:* methods: data analysis – methods: statistical – gamma rays: observations

### 1. INTRODUCTION

Of the 271 point sources of high-energy gamma-rays detected by the Energetic Gamma Ray Experiment Telescope (*EGRET*) on the Compton Gamma Ray Observatory spacecraft, most remain unidentified (Hartman et al. 1999). The nature of these sources is one of the biggest questions raised by the *EGRET* mission. Certainly some of them will turn out to belong to the established classes of sources: Active Galactic Nuclei (AGN) (Sowards-Emmerd et al. 2003; Willis 1996) and pulsars (Merck et al. 1996; Mukherjee et al. 1995; Yadigaroglu & Romani 1995). A few, as well, may be discovered to be artifacts of the Galactic diffuse emission. However there are more unidentified sources than expected from these populations (Merck et al. 1996). The large error regions for the *EGRET* sources often make it difficult to discern which of several candidates is the true counterpart in another wavelength.

When studying the unidentified sources, there are several observables which one might use to determine their nature. One can look at the spatial distribution (Grenier 1995; Kanbach et al. 1995) to estimate what fraction of the population is Galactic in nature, and what scale height the Galactic fraction has. One can look at positional correlations with other object types and Galactic structures (Esposito et al. 1996; Gehrels et al. 2000; Grenier 2000; Hartman et al. 1999; Kawasaki & Totani 2002; Mattox et al. 1997; Reimer et al. 2003; Romero et al. 1999;

Sturmer & Dermer 1995; Thompson et al. 1995; Torres et al. 2003; Walker et al. 2002; Wallace et al. 2002). The energy spectrum is another characteristic which can be used to classify sources as “pulsar-like”, “AGN-like”, or “other” (Merck et al. 1996).

In this same vein, one can examine the *EGRET* catalog sources for evidence of time variability, in hopes of distinguishing the various source classes. The known pulsars are seen to have a fairly constant flux ( $\pm < 10\%$  when averaged over many pulse periods, consistent with the systematic uncertainties in *EGRET* flux measurements), as is expected from the nature of their energy production. Many AGN are seen to flare dramatically, which makes their identification easier. But, as with many aspects of the *EGRET* data, it is difficult to characterize the time variability of most sources, because of the limited statistics and the non-continuous observations. Thus it is natural to look for a statistic which will measure the variability in a rigorous way.

This work is based on the dissertation of Tompkins (1999). Changes in the details of the method have caused changes in the numerical results, but the conclusions are not altered.

In §2 we briefly review the previous methods which have been used for evaluating the variability of *EGRET* point sources. In §3 we outline an improved method. In §4 we describe how this method was applied to the *EGRET* data. The results are described in §5 and summarized briefly in §6.

### 2. PREVIOUS METHODS

All previous analyses of the variability of *EGRET* sources have used the flux values published in the Second (Thompson et al. 1995) or Third *EGRET* Catalog

Electronic address: Patrick.Nolan@stanford.edu  
Electronic address: wtompkins@icarion.com  
Electronic address: isabelle.grenier@cea.fr  
Electronic address: peterm@leland.stanford.edu

(Hartman et al. 1999), hereafter called 2EG and 3EG. This introduces the problem of upper limits. Many of the individual observations produced no positive detections. For these observations, the flux is reported as a 95% confidence upper limit produced by LIKE, the standard *EGRET* likelihood program (Mattox et al. 1996).

The first comprehensive method used for estimating the variability of *EGRET* sources is the one introduced by McLaughlin et al. (1996). This method finds the  $\chi^2$  of the measured source intensities in 2EG, assuming a constant flux, and uses  $V = -\log Q$ , where  $Q$  is the tail probability of obtaining such a large  $\chi^2$ . There are two problems with this method: one statistical, and one conceptual. The statistical problem is introduced when using upper limits: McLaughlin et al. (1996) use zero as the flux estimate when the measured flux estimate would be negative, and for the error they use the LIKE upper limits. Thus their resulting “ $\chi^2$ ” will not have a  $\chi^2$  distribution. Since the LIKE results are statistically conservative, this means that sources with upper limits included in the analysis will have a lower  $V$  than they should. The conceptual problem with the  $V$  method is the use of a  $\chi^2$  statistic to determine variability. The  $Q$  statistic is the p-value for the hypothesis of constant source flux. Thus, sources with a large  $V$  are inconsistent with being constant. But we do not know whether such a source has a large  $V$  because of large intensity fluctuations, or because of small error bars on the intensity measurements. Similarly, a source with a small  $V$  might truly be constant, or it might just have very poor measurements of its flux.

Wallace et al. (2000) also applied this method to two-day segments of *EGRET* data, looking for rapid variation that would not have been discovered by examining full viewing periods. They were severely limited by large statistical uncertainties, but they found previously-undiscovered variation in several sources.

Torres et al. (2001a,b) describe a statistic called the  $I$  index.  $I$  is a normalized ratio of the standard deviation to the average flux. This is somewhat similar to the approach we describe below. It is a step toward dealing with the conceptual problem described above, but it introduces another ad-hoc approach to dealing with upper limits. Also there is no estimate of confidence intervals for  $I$  values.

Other, less quantitative criteria have been used to produce lists of sources which are not highly variable. These lists are heterogeneous collections of sources with rather different properties. In addition to truly non-variable sources, they tend to include bright variable sources. They exclude mainly the sources which flared once or twice and were otherwise undetectable. For instance, Grenier (2000) defined a class of 88 *persistent* unidentified sources. These are the ones which are significantly detected ( $> 4\sigma$  or  $> 5\sigma$ , depending on position) in the cumulative data up to 1995 October. Gehrels et al. (2000) produced a similar list of 120 *steady*, unidentified sources. They required that the flux in the cumulative data must be either a more significant detection than any individual observation or within  $3\sigma$  of the largest individual flux. Again the effects of average brightness and variability are hard to disentangle. It is difficult to compare sources or populations on the basis of these lists because they provide only a binary variable/nonvariable classification.

### 3. A LIKELIHOOD APPROACH

#### 3.1. What Do We Want to Measure?

We propose to answer two questions about the variability of a source: How much does the flux vary and how precisely do we know this? To do this we define

$$\delta \equiv \frac{\sigma}{\mu}, \quad (1)$$

where  $\mu$  and  $\sigma$  are the average and standard deviation, respectively, of the true flux of the source. This fractional variability is much closer to what we really want to know about a source. There could also be other statistics which might be more meaningful for flaring sources, such as the peak flare flux divided by the quiescent level. Since the flux measurements have uncertainties, we must find a way to estimate  $\delta$  from the data. Unfortunately this can't be done in a completely model-independent way.

#### 3.2. Modeling the Source Flux Distribution

We ignore the ordering and spacing of the individual flux measurements. We assume only that all flux values of a particular source are random values drawn from the same probability distribution. This approach eliminates all consideration of long timescale correlations in the data. The probability distribution is parameterized by  $\delta$ . Such a model is necessary in order to disentangle the effects of real flux variation from statistical fluctuations. An infinite number of source flux distributions exist which will yield the same  $\delta$ ; we want to pick one that is compatible with our notions of what the true source flux distribution should be, but which is also fairly general.

The first source flux distribution one might try is a Gaussian. Thus, we would find the likelihood of obtaining our data given that the true flux  $S$  was drawn from a Gaussian with mean  $\mu$  and standard deviation  $\sigma = \mu\delta$ . We could then find the maximum likelihood value of  $\delta$ , together with a confidence interval for  $\delta$  defined in the standard way (Eadie et al. 1971). Alternatively, we could follow the Bayesian procedure: form priors for the distributions of  $\mu$  and  $\delta$ , and find an estimate of  $\delta$ , together with an error region, by marginalizing over  $\mu$ . The use of the Gaussian distribution for source fluxes has a flaw, however. It allows the possibility of  $\mu = 0$  ( $\Rightarrow \delta = \infty$ ), as well as the unphysical possibility of negative  $\mu$ .

Instead of a Gaussian, we choose to use the gamma distribution; that is, the flux  $S$  is drawn from the differential probability distribution

$$P(S) = \frac{S^{\alpha-1} e^{-S/\beta}}{\beta^\alpha \Gamma(\alpha)}, \quad (2)$$

where the adjustable parameters  $\alpha (> 0)$  and  $\beta (> 0)$  describe the shape and scaling of the function, respectively. The parameters can be related to the desired quantities by  $\mu = \beta\alpha$ ,  $\sigma = \beta\sqrt{\alpha}$ , and  $\delta = \alpha^{-1/2}$ . This distribution function has a peak if  $\alpha > 1$ . For  $0 < \alpha < 1$ , it decreases monotonically from  $S = 0$ . This behavior is a good match for the different types of observed variations. Some sources are steady (large  $\alpha$ ), while many others are mostly faint with occasional flares (small  $\alpha$ ).

Tompkins (1999) did the same analysis described below using a lognormal distribution. There is an excellent correlation between the results, but the gamma distribution produced fewer numerical difficulties, such as lack of convergence. We take this as a validation of our choice of probability distribution.

#### 3.3. Characterizing the Single-Measurement Likelihood

It is standard in *EGRET* analysis to calculate the likelihood of the observed data for a certain source flux (Mattox et al.

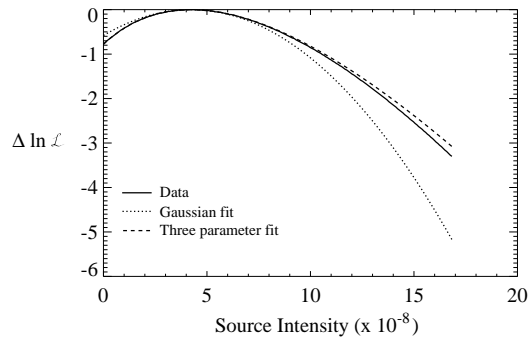


FIG. 1.— The likelihood curve for a sample source, together with a Gaussian of the same width, and a curve of the form in equation (3).

1996). Typically, the values output by an analysis program are the most likely flux and a confidence interval. In the case of upper limits, the most likely flux is taken as zero, and the confidence interval might be defined in one of several ways (Caso et al. 1998).

For this work, we would like to be able to calculate the likelihood for any source flux, not necessarily one near the maximum likelihood value. Thus it is useful to look for a parameterized family of curves which will closely fit the full likelihood function. The results of the many individual measurements can be stored in a compact form and reproduced quickly as needed.

After examining many such curves, we found a simple function which fulfills our requirements. We choose

$$\mathcal{L}(S) = e^{-(k+S/S_*)} (k + S/S_*)^p, \quad (3)$$

where  $S_*$ ,  $k$ , and  $p$  are adjustable parameters and only  $S \geq 0$  is allowed. A likelihood function need not be normalized. If  $p > k$ ,  $\mathcal{L}(S)$  has a peak at  $S = (p-k)S_*$  of width  $S_*\sqrt{p}$ , and the *EGRET* test statistic (Mattox et al. 1996)  $TS = 2p(k/p - \ln(k/p) - 1)$ . If  $p \leq k$ ,  $\mathcal{L}(S)$  has its maximum at  $S = 0$ . This function was originally derived by analogy with the Poisson probability function. The parameter  $p$  plays the role of an effective number of detected photons, while  $1/S_*$  is the exposure and the offset  $k$  accounts for the effects of diffuse emission and nearby point sources.  $\mathcal{L}(S)$  would become singular if  $k < 0$ , but this never occurred in our analysis.

This form fits the observed likelihood functions rather well (Figure 1), both in cases of large source flux and in upper limit situations.

### 3.4. Calculating Likelihood

With the parameterized distribution of source fluxes from the preceding section, we can use Bayes's Theorem to write the likelihood of observing a given viewing period's worth of data ( $D_i$ ) from a source with a certain  $\mu$  and  $\delta$ :

$$\mathcal{L}(\mu, \delta, D_i) = \int_0^\infty dS_i P(D_i|S_i) P(S_i|\mu, \delta) \quad (4)$$

$$= \int_0^\infty dS_i \mathcal{L}(S_i) P(S_i|\mu, \delta) \quad (5)$$

$$= \int_0^\infty dS_i e^{-(k_i+S_i/S_{*i})} (k_i + S_i/S_{*i})^{p_i} \times \frac{1}{(\mu\delta^2)^{1/\delta^2} \Gamma(1/\delta^2)} S_i^{(1/\delta^2-1)} e^{-S_i/(\mu\delta^2)}, \quad (6)$$

where the second term in equation (6) is the gamma distribution written in terms of  $\mu$  and  $\delta$ .

The likelihood of a sequence of observations ( $D_1 \dots D_M$ ) will then be

$$\mathcal{L}(\mu, \delta) = \prod_{i=1}^M \mathcal{L}(\mu, \delta, D_i),$$

or

$$\ln \mathcal{L}(\mu, \delta) = \sum_{i=1}^M \ln \mathcal{L}(\mu, \delta, D_i). \quad (7)$$

### 3.5. Dealing with Time Scales

We have assumed that the source flux during all the measurements was drawn independently from the same distribution. This can be problematic if the measurements last for varying lengths of time. For example, in the *EGRET* data, there are frequently several successive viewing periods of a few days duration, pointing in nearly the same direction. This is in contrast to the normal mode of pointing in one direction for two weeks at a time. We do not want our results to depend on whether or not a two week viewing period was chopped into several bits.

Our solution is to combine successive measurements if they occur within 30 days, and treat them as one measurement. Instead of the single-observation likelihood in equation (3), we use a composite  $\mathcal{L}(S)$  which is the product of the individual terms. The generalization of equation (6) is obvious. These combined measurements are reflected in the number of observations reported in Table 1.

Thus this analysis is sensitive to variations with a time scale of a month or more. We will not be able to detect the 1-2 day flares found by Wallace et al. (2000) from several *EGRET* sources.

## 4. ANALYSIS

### 4.1. Method

The first step in this analysis was the re-analysis of the 3EG catalog with a modified likelihood program which produces a likelihood function in the form of equation (3) (Tompkins 1999). For each Viewing Period, any of the 271 sources from 3EG Catalog which were within the instrument's field of view were included in the source list. In addition, any of the 145 marginal sources (which were used in the original analysis of the catalog but were not significant enough to merit inclusion in the official list) which were in the field of view were added as well. The maximum likelihood set of source fluxes was then found. For each source, the parameters characterizing  $\mathcal{L}(S)$  described in §3.3 were found. All source measurements were of flux ( $> 100$  MeV), assuming a spectral index of  $-2.0$ , using all photons within  $15^\circ$  of each source, and including all nearby sources (both catalog and marginal) in the model. We use only data taken with the full *EGRET* field of view, which includes everything through Viewing Period 429.0 (ending 1995 September 27) except for four periods (403.0, 403.5, 411.1, and 411.5). With the smaller field of view used to take the rest of the data, we are not confident that the detector response functions are calibrated well enough for our purpose. Also the number of point sources detected in each observation is reduced, so the remaining data are less useful. Results are used only for the point sources within  $25^\circ$  of the center of the field of view. This data selection is nearly the same as that used to produce the 3EG Catalog.

The likelihood of the sequence of observations as a function of  $\delta$  was then calculated, as in §3.4. All observations within one month of each other were lumped together, as per §3.5. From this likelihood, the most likely values of  $\delta$  were obtained, as well as confidence intervals. The mean flux  $\mu$  can be marginalized away as a nuisance parameter after checking that its most likely value is consistent with the 3EG flux.

#### 4.2. Sources Omitted from This Analysis

In the results reported below, several 3EG sources are omitted for various reasons.

Seven sources near the bright Crab and Vela pulsars are omitted because they are believed to be artifacts (Thompson et al. 2001): 3EG J0824–4610, 3EG J0827–4247, 3EG J0828–4954, 3EG J0841–4356, 3EG J0848–4429, 3EG J0859–4247, and 3EG J0521+2147.

The solar flare 3EG J0516+2320 is omitted because it is clearly a unique occurrence.

The sources 3EG J0829+2413 and 3EG J1424+3734 each had only one observation within  $25^\circ$  of the center of the field of view. Thus the variability of these sources can't be evaluated.

A cross-check of this analysis and the 3EG flux values turned up three sources with serious discrepancies: 3EG J0556+0409, 3EG J0628+1847, and 3EG J1310–0517. These three sources are omitted. The latter two are near very bright sources (Geminga and 3C279), so we believe that our modified likelihood program may become confused in such areas. It is encouraging that only these three sources fail this test. The consistency of results for all the others encourages us that the modified likelihood program is valid in the other cases.

#### 4.3. Systematic Errors

This analysis has two main sources of systematic error. The first is from the instrument itself. The sensitivity of the *EGRET* instrument is variable (Hartman et al. 1999; Thompson et al. 1995). Despite efforts to measure and compensate for long term drifts, there is a residual variability of about 10–11% (Esposito et al. 1999). In an effort to minimize this systematic error, only source observations within  $25^\circ$  of the instrument axis were used in the analysis.

It is conceivable that the variation in measured fluxes might be reduced by using the “noisy” measured sensitivity rather than the smoothed values that are usually employed in *EGRET* analysis. We tested this by calculating the fluxes of the three bright pulsars (Crab, Geminga, Vela) by both methods. With the measured sensitivity values, Vela appeared much more variable, the Crab slightly more, and Geminga slightly less. Thus it appears to be appropriate to continue using the smoothed sensitivities.

Because of the systematic variability, the Galactic and isotropic background levels  $G_M$  and  $G_B$  were allowed to vary from viewing period to viewing period for a given source in the likelihood analysis. Otherwise, a small change in a strong background could lead to a large change in a source flux. This procedure is standard practice for *EGRET* data analysis (Mattox et al. 1996).

The background levels were also allowed to float when  $\mathcal{L}(S)$  was calculated. Unfortunately, computational limitations precluded allowing nearby sources to vary during this calculation as well. Thus, nearby sources were fixed at their maximum likelihood intensities (calculated for that viewing period). This will lead to an underestimation of the error in flux,

particularly for sources which have another source very close by.

As both systematic effects will tend to exaggerate source variability, it is expected that even constant sources will show some small variability. To the extent that the systematics are dominated by the instrumental effects, the measured variability will be equal to the true variability added in quadrature to a constant systematic variability of about 10%.

#### 4.4. A Simple Variability Index

Although the most likely value of  $\delta$  and its confidence interval provide a good description of a source's variability, there is considerable interest in the simpler question of whether a source is variable at all, independent of the question “how much?” This is the goal of McLaughlin et al. (1996). This problem is complicated by the presence of the systematic errors. To help answer the question, we define the statistic  $V_{12}$ . It represents the confidence with which we can reject the hypothesis  $\delta < 0.12$ , where 0.12 is a conservative estimate of the average systematic error.

$$V_{12} \equiv -\log_{10}(1 - P_{\chi^2}(r|1)), \quad (8)$$

where

$$r = 2 \ln \frac{\mathcal{L}_{\max}(\mu, \delta)}{\mathcal{L}_{\max}(\mu, \delta = 0.12)}, \quad (9)$$

$\mathcal{L}_{\max}(\mu, \delta)$  is the unconstrained maximum likelihood,  $\mathcal{L}_{\max}(\mu, \delta = 0.12)$  is the maximum likelihood if  $\delta$  is constrained to equal the systematic value 0.12, and  $P_{\chi^2}(r|1)$  is the cumulative  $\chi^2$  probability distribution with one degree of freedom. The use of the  $\chi^2$  distribution can be justified by Wilks's Theorem (Cash 1979) when several independent likelihood functions are combined, even though they may not be Gaussian functions individually. If the most likely  $\delta$  is less than 0.12, then there is no estimate for  $V_{12}$ .  $V_{12}$  values greater than 16 are shown as  $\infty$  in Table 1. The p-value for rejecting the hypothesis that a source is non-variable is  $10^{-V_{12}}$ .

## 5. RESULTS

The results of this analysis are shown in Table 1. The columns in the table give the names in the 3EG catalog, the most likely Galactic longitudes and latitudes, the most likely values of  $\delta$ , the 68% lower and upper confidence limits on  $\delta$ ,  $V_{12}$ , the number of observations used in the analysis, possible associations with source classes, and specific identifications.

#### 5.1. Variability by Source Class

As can be seen from Table 1, the limits on the variability of an individual source are usually not very strict. By grouping similar sources together, one can learn more about the average behavior of a class of sources. There are many sources which are found in multiple classes. Many of the unidentified sources are found in densely-populated regions containing various types of young-population objects. The error boxes of the *EGRET* sources often contain several plausible counterparts. Table 2 shows the results for the various source classes. It contains a description of each class, the number of sources in the class, the mean of  $\delta$ , and an estimate of the intrinsic RMS dispersion of  $\delta$  in excess of the statistical errors. The last two quantities are calculated by assuming a Gaussian distribution for  $\delta$  and finding the likelihood as a function of mean and standard deviation by a method similar to that used in §4.1.

TABLE 2. VARIABILITY OF SELECTED CLASSES OF SOURCES

Source Class	Members	$\langle \delta \rangle$	RMS( $\delta$ )	Symbol
3EG Classification				
Pulsars	6	$0.11 \pm 0.02$	$< 0.07$	PSR
SNR associations	10	$0.27 \pm 0.09$	$< 0.19$	SNR
AGN (“A” in 3EG)	67	$0.70 \pm 0.08$	$0.27 \pm 0.05$	
Quasars	51	$0.77 \pm 0.09$	$0.25 \pm 0.08$	QSO
BL Lac objects	15	$0.49 \pm 0.16$	$< 0.32$	BLL
Unidentified, $ b  < 5^\circ$	47	$0.42 \pm 0.06$	$0.17 \pm 0.08$	U0
Unidentified, $5^\circ <  b  < 15^\circ$	37	$0.56 \pm 0.12$	$0.23 \pm 0.09$	U5
Unidentified, $15^\circ <  b  < 30^\circ$	45	$0.42 \pm 0.12$	$< 0.16$	U15
Unidentified, $ b  > 30^\circ$	29	$0.84 \pm 0.15$	$< 0.27$	U30
Possible isolated neutron stars				
Geminga-like objects	3	$0.13 \pm 0.11$	$< 0.16$	Gem
Pulsars without PWN	7	$0.21 \pm 0.15$	$< 0.15$	noPWN
Pulsars with PWN	6	$0.66 \pm 0.29$	$0.28 \pm 0.16$	PWN
Gould’s Belt, unidentified, $ b  > 5^\circ$	33	$0.49 \pm 0.13$	$< 0.26$	G
Persistent, unidentified (Gehrels et al. 2000)	88	$0.32 \pm 0.05$	$0.10 \pm 0.05$	Per
Steady, unidentified (Grenier 2000)	120	$0.35 \pm 0.05$	$0.11 \pm 0.04$	Std
Associations from Romero et al. (1999)				
SNR	17	$0.28 \pm 0.10$	$< 0.17$	RSN
WR stars	6	$0.45 \pm 0.22$	$< 0.27$	WR
Of stars	4	$0.26 \pm 0.15$	$< 0.19$	Of
OB associations	22	$0.40 \pm 0.10$	$0.17 \pm 0.08$	OB

To begin, consider four principal source classes based on the identifications in the 3EG catalog: Unidentified sources, Pulsars, Active Galactic Nuclei (AGN) (labeled “A” in 3EG), and sources which are spatially coincident with Supernova Remnants (SNR). The Unidentified source class was divided according to the Galactic latitude. These source classes were determined from the “source ID” (and by the “Other Name” category for the SNR associations) in the catalog. Also, 3EG J1048–5840 (PSR B1046–58) has been added as a sixth member of the pulsar class based on its recent detection (Kaspi et al. 2000). Although pulsations have been detected from PSR B1951+32 (Ramanamurthy et al. 1995), and reported from PSR B0656+14 (Ramanamurthy et al. 1996), they do not appear as detectable point sources in the 3EG catalog, so they are not considered here.

As seen in Table 2, the pulsars, AGN, and unidentified sources clearly differ in their variability. The variability of the six pulsars is about 11%, not significantly higher than the predicted systematic variability for a constant source of 10%.

When the firmly identified quasars and BL Lac objects are considered separately, a difference is clear. On the average, the BL Lacs are much less variable than the quasars. This confirms the observation made by Mukherjee et al. (1997).

The ten sources in the 3EG SNR source class are somewhat less variable than the low-latitude unidentified sources as a whole, and show significantly more variation than the pulsar class. Of course, it is by no means certain that these sources are supernova remnants. They are found in crowded areas of the sky along with other types of objects characteristic of star-forming regions (Yadigaroglu & Romani 1997). Romero et al. (1999) identify 17 possible SNR associations, of which 7 are also in the 3EG SNR list. These two SNR collections have very similar variability properties. If the gamma rays are produced in a large region of the SNR, then the flux should be steady. Observable variation would be an indication of gamma production in a pulsar wind or perhaps of the presence of a background blazar.

The change in unidentified source variability with latitude can be seen in Table 2. It is clear from the spatial dis-

tribution of the unidentified sources that there are multiple types of astrophysical objects which have not been identified (Gehrels et al. 2000; Grenier 1995; Kanbach et al. 1995). It is clear that the different types of unidentified sources have different variabilities as well. The high latitude sources have a variability index consistent with that of the identified AGN, and many of them have plausible AGN counterparts (Mattox et al. 2001, 1997; Sowards-Emmerd et al. 2003). The low latitude unidentified sources exhibit some variability, at a level a little more than the sources coincident with SNR.

In the literature a number of other possible associations with source classes have been suggested, not based on the classifications in the 3EG catalog. Table 2 also summarizes the properties of these classes.

Grenier (2003) listed 13 3EG sources with positions consistent with radio pulsars and reasonable  $L_\gamma/\dot{E}$  ratios. Six of these (3EG J1013–5915, 3EG J1420–6038, 3EG J1837–0423, 3EG J1856+0114, 3EG J2021+3716, 3EG J2227+6122) have pulsar wind nebulae (PWN) which might be significant gamma sources. (3EG J1410–6147 is not counted as a PWN source because it can be associated with two pulsars, but the one with a PWN can be discounted on energetic grounds.) The seven non-PWN sources (3EG J1014–5705, 3EG J1102–6103, 3EG J1410–6147, 3EG J1639–4702, 3EG J1714–3857, 3EG J1824–1514, 3EG J1837–0606) have an average  $\delta$  of  $0.21 \pm 0.15$ , while the six PWN sources have an average  $\delta$  of  $0.66 \pm 0.29$ . These numbers suggest that most of the associations are correct and that PWNs can be strong, variable gamma emitters. Three of the PWN sources are among the variable Galactic plane sources in §5.4.

Four of the identified gamma-ray pulsars are known to have wind nebulae: Crab, Vela, PSR B1046–58, and PSR B1706–44. Their gamma emission is clearly dominated by the pulsars. Any variation in the nebular output in the  $> 100$  MeV band is hidden from this analysis. The Crab Nebula, for instance, is variable on a scale of years (de Jager et al. 1996), but the changes can be seen only in a certain energy band, and only in the off-pulse emission. Note: We do not con-

sider the complex source 3EG J0222+4253 here because of the confusion of emission from its pulsar and blazar counterparts (Hartman et al. 1999).

Three other 3EG sources have plausible associations with isolated neutron stars. They have hard spectra, large gamma to X-ray flux ratios, and no known pulsar counterparts, so they might be Geminga-class objects: 3EG J0010+7309 (Brazier et al. 1998), 3EG J1835+5918 (Chandler et al. 2001; Mirabal & Halpern 2001; Reimer et al. 2001), and 3EG J2020+4017 (Brazier et al. 1996). Individually they show little sign of variability. As a class, their average  $\delta$  is  $0.13 \pm 0.11$ , quite consistent with the identified pulsars.

Grenier (2000) suggested an association of *EGRET* sources with Gould’s Belt. Perrot & Grenier (2003) produced a model of the Belt based on a 3D simulation of Galactic dynamics. There are 47 unidentified 3EG sources whose positions are consistent with their model. Of these, four are omitted from this analysis as described in §4.2. Ten more are at  $|b| < 5^\circ$ , so they are likely to be contaminated by the Galactic plane population(s). The remaining 33 have an average  $\delta$  of 0.49. This is a moderately low value, but these sources as a class are definitely more variable than the pulsars. Perhaps a fraction of them are Myr-old pulsars (Harding & Zhang 2001).

Romero et al. (1999) made lists of possible associations with very young objects: WR stars, Of stars, and OB associations. These all have an average  $\delta$  of 0.26 to 0.45, fairly steady but more variable than pulsars.

It has been proposed (Colafrancesco 2002; Kawasaki & Totani 2002) that some high-latitude *EGRET* sources may be galaxy clusters which produce gamma rays in their intracluster gas. Of course such a source would be non-variable on a scale of months to years. Kawasaki & Totani (2002) picked a sample of seven *EGRET* sources, chosen on the basis of steady emission and other criteria. 3EG J1310–0517 is omitted from our analysis, and the other six show no significant evidence of variation. The upper limits on  $\delta$  are not tight (0.86 to 1.30), so the non-variability of these sources is an open question. Colafrancesco (2002) has a list of nine probable associations, three of which are also in the Kawasaki & Totani (2002) list. However, he includes 3EG J0253–0345 and 3EG J0215+1123. Both of those are variable.

As described in §2, Gehrels et al. (2000) produced a list of 120 “steady” sources and Grenier (2000) a list of 88 “persistent” sources. Most of the “persistent” sources are also in the “steady” list. These lists were attempts to eliminate strongly flaring sources and ones which are only marginally detectable. Apparently they succeeded, since the mean  $\delta$  values (0.32 and 0.35) are fairly low. However, there are several examples of clearly variable sources in these lists.

### 5.2. The Lowest Variability Sources

With the variability of the source classes in hand, it is possible to see which sources can be excluded from a source class based on the variability data. We begin by examining those sources which are inconsistent with being strongly variable: that is, the upper bound ( $\delta_{\max}$ ) of the 68% region for  $\delta$  is small. There are 8 sources for which this upper bound is less than 0.4, significantly lower than the typical value for AGN or unidentified sources.

Five of the six pulsars are in the list, with PSR B1055–52 barely excluded. The possibility that others on the list might also be pulsars is intriguing. The sources are discussed indi-

vidually below.

The position of the Crab pulsar 3EG J0534+2200, at the top of the list, is a bit surprising given its listing in McLaughlin et al. (1996) as moderately variable. There are two reasons for this. The first is the difference in the methods: McLaughlin et al. report the confidence level with which the hypothesis of steady emission can be rejected. In their analysis, the bright Crab, Geminga, and Vela pulsars are all inconsistent with being constant at the 95% level due to systematic errors and the small statistical uncertainties. The second reason is the difference in data used: McLaughlin et al. used all measurements up to to  $30^\circ$  from the instrument axis. In this analysis, we have used only data out to  $25^\circ$ , because of the larger systematic errors at higher inclinations.

3EG J1048–5840 is coincident with PSR B1046–58, a high  $\dot{E}/d^2$  pulsar. Although pulsed emission was not seen in the first three years of *EGRET* data (Fierro 1995), there has been a detection in more recent data (Kaspi et al. 2000).

3EG J0222+4253 is coincident with the BL Lac 3C 66A, and is  $1^\circ$  from the position of PSR J0218+4232, from which pulsed emission above 100 MeV has been reported (Kuiper et al. 2002; Kuiper et al. 2000; Verbunt et al. 1996). In the 3EG catalog, the pulsar was not detected as a separate source, and it is suggested that the flux between 100 MeV and 1 GeV is primarily from the pulsar, while the flux above 1 GeV is mostly from 3C 66A (Hartman et al. 1999). The flux measurements of this “source” will be dominated by the lower energy emission, hence the low variability. Wallace et al. (2000) found a significant variation of this “source” on a 2-day timescale, likely from the AGN. Since our analysis uses only full observations, we can’t confirm or reject this variation.

The  $\delta$  value of the Vela pulsar 3EG J0834–4511 is slightly higher than the 10% systematic variation. This is due to the presence of several artifact sources nearby (Thompson et al. 2001). In a few viewing periods, the measured flux of Vela is low, and the flux from an artifact is quite high. Because nearby source fluxes were not re-fit for each point on the likelihood-vs-intensity curve, such “flux leaking” can lead to an apparently high variability. By fixing the fluxes of the spurious sources one could lower Vela’s variability, but only if those nearby sources were not themselves variable. This was not done because of the unknown biases that could result.

3EG J2020+4017 is unidentified, but its position is coincident with the  $\gamma$ -Cyg supernova remnant, so it is thus an intriguing pulsar candidate. No pulsed signal has been detected from it, however, and the possibility exists that it is a radio-quiet pulsar (Brazier et al. 1996; Chandler et al. 2001).

3EG J1734–3232, another unidentified source, is the last member of this group.

It is noteworthy that 3EG J0721+7120 almost qualifies for this list. It is identified in the 3EG Catalog as the BL Lac object 0716+714 (Hartman et al. 1999; von Montigny et al. 1995; Mukherjee et al. 1997). The upper end of the 68% confidence region for  $\delta$  is 0.38, well below the typical AGN variability of  $\sim 0.7$ . In large part, this is because this source had no dramatic flares during any observations. In addition, the viewing periods with the highest and lowest fluxes were each combined with less extreme observations by the one-month averaging system (§4.1, §3.5). A more sophisticated model might pick up longer or shorter term trends.

### 5.3. The Highest Variability Sources

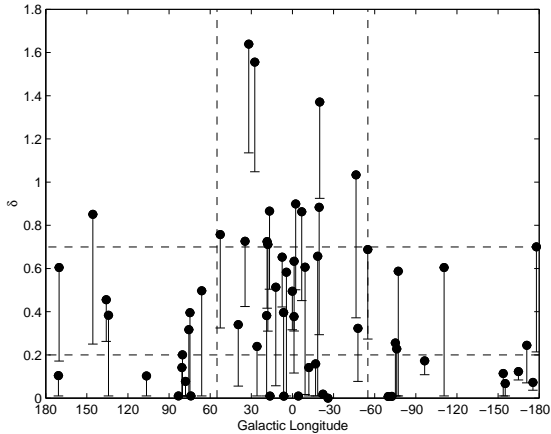


FIG. 2.— Values of  $\delta$ , a measure of variability, for gamma sources within  $\pm 6^\circ$  of the Galactic Plane. For each source, the filled circle is the most likely value of  $\delta$  and the lower end of the bar is  $\delta_{\min}$ , the 68% confidence lower limit. The vertical dashed lines are drawn at longitudes of  $\pm 55^\circ$  to guide the eye. The horizontal lines are at the arbitrarily chosen cutoff values for variable sources: 0.7 for the most likely  $\delta$  and 0.2 for  $\delta_{\min}$ . All of the highly variable sources are within the central region of the Galaxy.

From Table 1, 18 sources have a 68% confidence region with a lower bound greater than 0.7. These include 11 sources identified as AGN. Four of the unidentified sources (3EG J1227+4302, 3EG J1607–1101, 3EG J2006–2321, and 3EG J2251–1341) are at high Galactic latitudes, and are generally believed to be AGN (Hartman et al. 1999; Mattox et al. 2001; Wallace et al. 2002). The three remaining low latitude, unidentified sources are 3EG J1704–4732, 3EG J1828+0142, and 3EG J1837–0423. Halpern et al. (2003) and Sowards-Emmerd et al. (2003) propose a blazar identification for 3EG J1828+0142. Tavani et al. (1997) discovered the variability of 3EG J1837–0423, but they reject a blazar identification. None of the seven unidentified sources is classified as steady or persistent.

Because the  $V$  statistic used by McLaughlin et al. (1996) indicates how improbable it is that the observations come from a constant source, the use of the  $\delta$  statistic in this way is nearly equivalent to the use of  $V$  to find variable sources. Indeed, when there is a close correspondence between 2EG and 3EG sources, sources with a high  $V$  also have a high lower limit on  $\delta$ .

#### 5.4. Galactic Plane Sources

It is interesting to examine the behavior of the gamma sources near the Galactic plane. There are many which show no sign of variability, but there are some variable sources which are distributed non-uniformly in Galactic longitude. Figure 2 shows  $\delta$  values for the 66 sources within  $6^\circ$  of the Galactic plane. If we define a variable source as one with a most likely  $\delta$  value  $> 0.7$  or a minimum  $\delta > 0.2$ , then it can be seen that almost all of the 17 variable, low-latitude sources are clumped within  $55^\circ$  of the Galactic center. All 17 are unidentified.

Figure 3 shows histograms of the most likely  $\delta$  values for all the sources within  $6^\circ$  of the Galactic plane. The dashed line shows the  $\delta$  distribution for the sources with  $|\ell| < 55^\circ$ , while the solid line shows the others. A Kolmogorov-Smirnov test (Eadie et al. 1971) rejects the hypothesis that these two sets of values are drawn from the same population with a p-value of 5.1%.

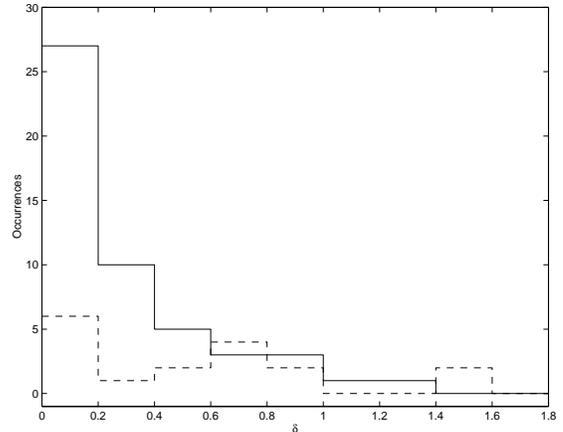


FIG. 3.— Distributions of most likely  $\delta$  values for sources within  $6^\circ$  of the Galactic plane. Dashed line: Sources within  $55^\circ$  longitude of the Galactic center. Solid line: Other sources.

Figure 2 shows values of  $\delta$  for these sources as a function of longitude. The filled circles show the most likely  $\delta$  values and the ends of the bars show 68% confidence lower limits ( $\delta_{\min}$  in Table 1). The horizontal dashed lines are drawn at  $\delta = 0.7$  and  $\delta_{\min} = 0.2$  to guide the eye.

Some of the apparent variation might be due to flux leakage between close companions, as with the Vela pulsar (§5.2). Among the 17 variable sources there are three pairs and a triple within a few degrees. No pair of these sources has correlated fluxes with a correlation coefficient  $> 0.18$ , except 3EG J1823–1314 and 3EG J1826–1302. Their correlation coefficient is  $-0.41$ , with a p-value of 2.4%. The variation of these two sources might be spurious, but the others seem to be on more solid ground.

The distribution of variable sources is consistent with a young Galactic population, as traced by molecular clouds (Dame et al. 2001), OB associations (Kaaret & Cottam 1996), SNRs and HII regions (Sturmer & Dermer 1995; Sturmer et al. 1996; Yadigaroglu & Romani 1997), WR stars and Of stars (Romero et al. 1999). The concentration in the inner radian and their latitude spread indicate typical distances of 5–8 kpc and luminosities  $L(E > 100 \text{ MeV}, 4\pi \text{ sr})$  of  $(1-25) \times 10^{35} \text{ (D/5 kpc)}^2 \text{ erg s}^{-1}$ . This is slightly higher than the range found by Kanbach et al. (1995) for all the low-latitude sources in the 2EG catalog, both variable and non-variable.

This luminosity range is typical of X-ray binaries and 10 kyr-old pulsars. The latter are expected to be steady emitters, but variable emission from pulsar wind nebulae is possible. In particular, plerionic activity is more likely to explain the hard but variable 3EG J1856+0114 source than pulsed emission from the 20 kyr-old pulsar or cosmic-ray emission in the surrounding W44 supernova shell. The same may be true for 3EG J1420–6038 in the Kookaburra nebula and 3EG J1837–0423 near the G27.8+0.6 plerion. 3EG J1809–2328 also coincides with a pulsar wind nebula, but inverse-Compton emission from electrons scattering the nebular synchrotron emission or the ambient radiation field from the nearby OB association fail to explain the source brightness (Braje et al. 2002). A 21 kyr-old pulsar, PSR J1826–1334, found near the edge of the 3EG J1826–1302 error box, could power the gamma-ray source. Pulsars are also found near 3EG J1308–6112 and 3EG J1928+1733, but they are much too weak to explain the

sources.

Variability over months is common in accreting systems. One high-mass X-ray binary, GX 304–1, hosting a Be star and a neutron star on an eccentric 132.5-day orbit, is found toward 3EG J1308–6112. It is known to exhibit strong long-term variability in X rays. Electrons accelerated at the shock between the pulsar and stellar winds have been proposed to shine up to TeV energies by upscattering the stellar radiation (Kirk et al. 1999; Tavani & Arons 1997), but the 272 s pulsar in GX 304–1 is not likely to power a strong, energetic wind. 3EG J1736–2908 coincides with the X-ray source GRS 1734–292, which has been recently identified as a nearby Seyfert 1 galaxy ( $Z = 0.0214$ ) with radio jet emission and hard X-ray emission up to 400 keV (Marti et al. 1998). Confirmation of variable emission above 100 MeV from this galaxy would yield a first example of the activity of a Seyfert jet at high energy and suggest a valuable target for TeV telescopes.

Curiously, 11 of the 17 variable sources are in the “steady” category, and 10 are “persistent.” This happens because they are fairly bright. As long as they don’t vanish entirely for many observations, they still meet the selection criteria.

### 5.5. The Galactic Center

The source nearest to the Galactic center, 3EG J1746–2851, seems to be one of these variable sources. Mayer-Hasselwander et al. (1998) found only weak evidence that this source might be variable. With more data and a more sensitive method, the statistical evidence of its variability is fairly strong ( $V_{12} = 2.35$ ). This would rule out any model in which this object is a cluster of neutron stars, a condensation of dark matter particles, or other non-compact object (Bertone et al. 2003; Calcáneo-Roldán & Moore 2000; Cesarini et al. 2003; Markoff et al. 1999; Mayer-Hasselwander et al. 1998; Pohl 1997).

This conclusion is reinforced by Hooper & Dingus (2003), who show that the position of the *EGRET* source is not consistent with the Galactic Center. 3EG J1746–2851 may be a field source like the other 16 low-latitude variables. The probability of such a chance positional coincidence near the Galactic Center is about 2.7%.

Since the diffuse emission is most intense in the neighborhood of the Galactic Center, it is conceivable that errors in the background model or instrument PSF will have their greatest effect there. To check this we correlated the flux of 3EG J1746–2851 with the angle to the instrument pointing direction. The correlation coefficient is 0.46, which has a p-value of 1.5%. If the maximum viewing angle is reduced from  $25^\circ$  to  $17^\circ$ , seven observations are eliminated. The flux-angle correlation is reduced to an insignificant level, but the estimate of  $\delta$  becomes consistent with zero.

If there is a systematic problem at the Galactic Center, it should show up also in measurements of nearby sources. There are four other sources within  $6^\circ$  of the Center: 3EG J1734–3232, 3EG J1736–2908, 3EG J1741–2312, and 3EG J1744–3011. None of them shows such a large correlation of viewing angle and flux, and in one case the correlation is negative.

However, 3EG J1741–2321 and 3EG J1744–3011 have a substantial negative flux correlation ( $-0.33$  and  $-0.42$  respectively) with 3EG J1746–2851. This might be a sign of flux leakage, although 3EG J1741–2312 is rather far away.

In view of these somewhat ambiguous signs of extra sys-

tematic errors, we must declare that the variability of 3EG J1746–2851 is only a tentative conclusion.

## 6. CONCLUSIONS

It is possible to characterize the flux variation of *EGRET* gamma-ray sources between viewing periods in a consistent way by using a simple model for the flux distribution and combining likelihood functions. This method produces useful results for almost all of the sources in the Third *EGRET* catalog, using both positive detections and upper limits in a uniform manner. The resulting table displays the average fractional variation  $\delta$  and its confidence interval. For faint sources the confidence interval is necessarily large, allowing a wide range of possible behaviors.

The identified rotation-powered pulsars all show a small variability, consistent with the estimated 10% systematic errors in the flux measurements. In general, identified blazars are highly variable, although there are a few exceptions. The unidentified sources show a range of behaviors. Their average variability increases with Galactic latitude, indicating that there are multiple populations. Unidentified sources associated with pulsar with wind nebulae are, as a class, more variable than the ones associated with pulsars without nebulae. The highest-latitude unidentified sources have an average behavior similar to blazars.

There is a population of 17 highly-variable sources along the Galactic plane. These are concentrated in longitude within 1 radian of the Galactic center. This is probably a high-luminosity population of sources in the inner spiral arms and molecular ring, while the remaining less-variable sources are closer and less luminous.

This work was supported by NASA grant NAG5-1605 and the ARCS Foundation. The authors acknowledge helpful discussions with David Thompson, Mallory Roberts, Olaf Reimer, Robert Hartman, and Brian Jones. This research has made use of NASA’s Astrophysics Data System and the SIMBAD database, operated at CDS, Strasbourg, France.

## REFERENCES

- Bertone, G., Sigl, G., & Silk, J. 2003, *MNRAS*, 337, 98
- Braje, T. M., Romani, R. W., Roberts, M. S. E., & Kawai, N. 2002, *ApJ*, 565, L91
- Brazier, K. T. S., Kanbach, G., Carramiñana, A., Guichard, J., & Merck, M. 1996, *MNRAS*, 281, 1033
- Brazier, K. T. S., Reimer, O., Kanbach, G., & Carramiñana, A. 1998, *MNRAS*, 295, 819
- Calcáneo-Roldán, C. & Moore, B. 2000, *Phys.Rev.D*, 62, 123005
- Cash, W. 1979, *ApJ*, 228, 939
- Caso, C. et al. 1998, *European Physical Journal*, C3, 1
- Cesarini, A., Fucito, F., Lionetto, A., Morselli, A., & Ullio, P. 2003, *Astropart. Phys.*, submitted, preprint (astro-ph/0305075)
- Chandler, A. M., Koh, D. T., Lamb, R. C., Macomb, D. J., Mattox, J. R., Prince, T. A., & Ray, P. S. 2001, *ApJ*, 556, 59
- Colafrancesco, S. 2002, *A&A*, 396, 31
- Dame, T. M., Hartman, D., & Thaddeus, P. 2001, *ApJ*, 547, 792
- de Jager, O. C., Harding, A. K., Michelson, P. F., Nel, H. I., Nolan, P. L., Sreekumar, P., & Thompson, D. J. 1996, *ApJ*, 457, 253
- Eadie, W. T., Drijard, D., James, F. E., Roos, M., & Sadoulet, B. 1971, *Statistical Methods in Experimental Physics* (Amsterdam: North-Holland)
- Esposito, J. A. et al. 1996, *ApJ*, 461, 820
- . 1999, *ApJS*, 123, 203
- Fierro, J. M. 1995, PhD thesis, Stanford University, available at <http://giants.stanford.edu/~jmf/thesis/>
- Gehrels, N., Macomb, D. J., Bertsch, D. L., & Hartman, R. C. 2000, *Nature*, 404, 363
- Grenier, I. A. 1995, *Adv. Space Res.*, 15, 73
- . 2000, *A&A*, 364, L93
- Grenier, I. A. 2003, in *Texas in Tuscany: XXI Symposium on Relativistic Astrophysics* (Singapore: World Scientific), preprint (astro-ph/0303498)
- Halpern, J. P., Eracleous, M., & Mattox, J. R. 2003, *AJ*, 125, 572
- Harding, A. K. & Zhang, B. 2001, *ApJ*, 548, L37
- Hartman, R. C. et al. 1999, *ApJS*, 123, 79
- Hooper, D. & Dingus, B. L. 2003, *Phys.Rev.Lett*, submitted, preprint (astro-ph/0210617)
- Kaaret, P. & Cottam, J. 1996, *ApJ*, 462, L35
- Kanbach, G. et al. 1995, *A&AS*, 120, C461
- Kaspi, V. M., Lackey, J. R., Mattox, J., Manchester, R. N., Bailes, M., & Pace, R. 2000, *ApJ*, 528, 445
- Kawasaki, W. & Totani, T. 2002, *ApJ*, 576, 679
- Kirk, J. G., Ball, L., & Skjaeraasen, O. 1999, *Astroparticle Phys.*, 10, 31
- Kuiper, L., Hermsen, W., Verbunt, F., Ord, S., Stairs, I., & Lyne, A. 2002, *ApJ*, 577, 917
- Kuiper, L., Hermsen, W., Verbunt, F., Thompson, D. J., Stairs, I. H., Lyne, A. G., Strickman, M. S., & Cusumano, G. 2000, *A&A*, 359, 615
- Markoff, S., Melia, F., & Sarcevic, I. 1999, *ApJ*, 522, 870
- Marti, J., Mirabel, I. F., Chaty, S., & Rodríguez, L. F. 1998, *New Astronomy Review*, 42, 621
- Mattox, J. R., Hartman, R. C., & Reimer, O. 2001, *ApJS*, 135, 155
- Mattox, J. R., Schachter, J., Molnar, L., Hartman, R. C., & Patnaik, A. R. 1997, *ApJ*, 481, 95
- Mattox, J. R. et al. 1996, *ApJ*, 461, 396
- Mayer-Hasselwander, H. A. et al. 1998, *A&A*, 335, 161
- McLaughlin, M. A., Mattox, J. R., Cordes, J. M., & Thompson, D. J. 1996, *ApJ*, 473, 763
- Merck, M. et al. 1996, *A&AS*, 120, C465
- Mirabal, N. & Halpern, J. P. 2001, *ApJ*, 547, L137
- von Montigny, C. et al. 1995, *ApJ*, 440, 525
- Mukherjee, R., Bertsch, D. L., Dingus, B. L., Kanbach, G., Kniffen, D. A., Sreekumar, P., & Thompson, D. J. 1995, *ApJ*, 441, L61
- Mukherjee, R. et al. 1997, *ApJ*, 490, 116
- Perrot, C. A. & Grenier, I. A. 2003, *A&A*, 404, 519
- Pohl, M. 1997, *A&A*, 317, 441
- Ramanamurthy, P. V., Fichtel, C. E., Harding, A., Kniffen, D. A., Sreekumar, P., & Thompson, D. J. 1996, *A&AS*, 120, C115
- Ramanamurthy, P. V. et al. 1995, *ApJ*, 447, L109
- Reimer, O., Brazier, K. T. S., Carramiñana, A., Kanbach, G., Nolan, P. L., & Thompson, D. J. 2001, *MNRAS*, 324, 772
- Reimer, O., Pohl, M., Sreekumar, P., & Mattox, J. R. 2003, *ApJ*, 588, 155
- Romero, G. E., Benaglia, P., & Torres, D. F. 1999, *A&A*, 348, 868
- Sowards-Emmerd, D., Romani, R. W., & Michelson, P. F. 2003, *ApJ*, 590, 109
- Sturmer, S. J. & Dermer, C. D. 1995, *A&A*, 293, L17
- Sturmer, S. J., Dermer, C. D., & Mattox, J. R. 1996, *A&AS*, 120, C445
- Tavani, M. & Arons, J. 1997, *ApJ*, 477, 439
- Tavani, M., Mukherjee, R., Mattox, J. R., Halpern, J., Thompson, D. J., Kanbach, G., Hermsen, W., Zhang, S. N., & Foster, R. S. 1997, *ApJ*, 479, L109
- Thompson, D. J., Bertsch, D. L., & Hartman, R. C. 2001, in "Gamma 2001", ed. S. Ritz, N. Gehrels, & C. R. Shrader, AIP Conf. Proc. 587 (Melville, NY: AIP), 668
- Thompson, D. J. et al. 1995, *ApJ*, 101, 259
- Tompkins, W. F. 1999, PhD thesis, Stanford University, available at <http://giants.stanford.edu/~billt/thesis.ps>
- Torres, D. F., Pessah, M. E., & Romero, G. E. 2001a, *Astron. Nachr.*, 322, 223
- Torres, D. F., Romero, G. E., Combi, J. A., Benaglia, P., Andernach, H., & Punsly, B. 2001b, *A&A*, 370, 468
- Torres, D. F., Romero, G. E., Dame, T. M., Combi, J. A., & Butt, Y. M. 2003, *Adv. Space Res.*, in press, preprint (astro-ph/0301424)
- Verbunt, F., Kuiper, L., Belloni, T., Johnston, H. M., de Bruyn, A. G., Hermsen, W., & van der Klis, M. 1996, *A&A*, 311, L9
- Walker, M., Mori, M., & Ohishi, M. 2002, *ApJ*, 589, 810
- Wallace, P. M., Griffis, N. J., Bertsch, D. L., Hartman, R. C., Thompson, D. J., Kniffen, D. A., & Bloom, S. D. 2000, *ApJ*, 540, 184
- Wallace, P. M., Halpern, J. P., Magalhães, A. M., & Thompson, D. J. 2002, *ApJ*, 569, 36
- Willis, T. D. 1996, PhD thesis, Stanford University, available at <ftp://razzle.stanford.edu/pub/tdw/Thesis.ps.z>
- Yadigaroglu, I.-A. & Romani, R. W. 1995, *ApJ*, 449, 211
- . 1997, *ApJ*, 476, 347

TABLE 1. VARIABILITY  $\delta$  OF SOURCES IN THE THIRD *EGRET* CATALOG

3EG Name	$\ell$ (deg)	b (deg)	$\delta$	$\delta_{\min}$	$\delta_{\max}$	$V_{12}$	Num Obs	Classes	ID
J0010+7309	119.92	+10.54	0.26	0	0.73	0.40	3	U5,SNR,Std,Pst,Gem	CTA 1
J0038-0949	112.69	-72.44	0	0	1.34	...	3	U30,Std,Pst	
J0118+0248	136.23	-59.36	1.18	0.48	2.18	1.64	4	a	0119+041
J0130-1758	169.71	-77.11	0	0	0.63	...	4	a	0130-171
J0159-3603	248.89	-73.04	0	0	0.85	...	3	U30,Std,Pst	
J0204+1458	147.95	-44.32	1.29	0.60	2.54	2.62	3	QSO	0202+149
J0210-5055	276.10	-61.78	0.31	0.15	0.57	1.26	6	QSO	0208-512
J0215+1123	153.75	-46.37	1.27	0.59	2.48	2.10	3	U30	
J0222+4253	140.14	-16.77	0	0	0.37	...	4	BLL	3C 66A, PSR J0218+4232
J0229+6151	134.20	+1.15	0	0	0.51	...	5	U0,Of,OB,G,Std,Pst	
J0237+1635	156.77	-39.11	0.89	0.46	1.89	5.07	3	BLL	0235+164
J0239+2815	150.21	-28.80	0	0	0.41	...	5	a	0234+285
J0241+6103	135.87	+0.99	0.38	0.17	0.79	1.41	5	U0,G,Std,Pst	
J0245+1758	157.62	-37.11	1.14	0.44	2.16	1.38	4	U30,Std	
J0253-0345	179.70	-52.56	1.34	0.63	2.98	2.03	2	U30	
J0323+5122	145.64	-4.67	0.92	0.31	1.68	1.26	7	U0,G,Std	
J0329+2149	164.90	-27.88	0	0	1.55	...	5	U15,Std	
J0340-0201	188.00	-42.45	0	0	1.24	...	2	QSO	0336-019
J0348+3510	159.06	-15.01	0.45	0	1.29	0.24	6	U15,G,Std,Pst	
J0348-5708	269.35	-46.79	1.19	0	1.86	0.79	8	U30	
J0404+0700	184.00	-32.15	0.39	0	1.53	0.11	6	U30,Std,Pst	
J0407+1710	175.63	-25.06	0.90	0	1.59	0.55	9	U15,G,Std	
J0412-1853	213.90	-43.29	0	0	2.10	...	2	QSO	0414-189
J0416+3650	162.22	-9.97	0.59	0.10	1.15	0.89	9	a	0415+379
J0422-0102	194.88	-33.12	0	0	1.08	...	4	QSO	0420-014
J0423+1707	178.48	-22.14	0.42	0	1.02	0.42	10	U15,G,Std,Pst	
J0426+1333	181.98	-23.82	0	0	0.73	...	12	U15,G,Std,Pst	
J0429+0337	191.44	-29.08	0	0	0.73	...	8	U15,Std,Pst	
J0433+2908	170.48	-12.58	0.40	0.10	0.75	0.82	11	QSO	0430+2859
J0435+6137	146.50	+9.50	0	0	0.54	...	6	U5,Std,Pst	
J0439+1105	186.14	-22.87	0	0	0.74	...	12	U15,G,Std,Pst	
J0439+1555	181.98	-19.98	1.08	0.48	1.63	1.20	12	U15,G	
J0442-0033	197.20	-28.46	1.59	1.12	2.31	14.59	8	QSO	0440-003
J0450+1105	187.86	-20.62	1.13	0.78	1.64	8.42	12	QSO	0446+112
J0456-2338	223.96	-34.98	0.21	0	1.42	0.05	5	QSO	0454-234
J0458-4635	252.40	-38.40	0.41	0	1.19	0.23	6	QSO	0454-463
J0459+0544	193.99	-21.66	0.74	0	1.43	0.54	10	QSO	0459+060
J0459+3352	170.25	-5.77	0.59	0.14	1.18	0.95	12	U5,G,Std,Pst	
J0500+2529	177.18	-10.28	0	0	1.22	...	12	U5,G	
J0500-0159	201.35	-25.47	1.09	0.58	1.71	2.29	9	QSO	0458-020
J0510+5545	153.99	+9.42	0	0	0.41	...	7	U5,Std,Pst	
J0512-6150	271.25	-35.28	0	0	0.71	...	8	a	0506-612
J0520+2556	179.65	-6.40	0	0	0.53	...	12	U5,G,Pst	
J0530+1323	191.37	-11.01	0.74	0.55	1.05	$\infty$	13	QSO	0528+134
J0530-3626	240.94	-31.29	0.58	0	1.75	0.56	3	a	0521-365
J0531-2940	233.44	-29.31	0.85	0	1.91	0.60	4	a	0537-286
J0533+4751	162.61	+7.95	0	0	0.51	...	8	U5,Std,Pst	
J0533-6916	279.73	-32.09	0.29	0	0.79	0.13	8		LMC
J0534+2200	184.56	-5.78	0.08	0.03	0.15	...	12	PSR	Crab
J0540-4402	250.08	-31.09	0.75	0.46	1.27	6.18	6	BLL	0537-441
J0542+2610	182.02	-1.99	0.57	0	1.17	0.76	12	U0,SNR,RSN	S147
J0542-0655	211.28	-18.52	1.38	0.84	2.14	1.93	7	a	0539-057
J0546+3948	170.75	+5.74	0.10	0	0.68	...	11	U5,Std,Pst	
J0613+4201	171.32	+11.40	0.72	0.09	1.38	0.87	10	U5,Std,Pst	
J0616-0720	215.58	-11.06	0	0	1.32	...	8	U5,G,Std	
J0616-3310	240.35	-21.24	0.17	0	1.04	0.04	3	U15,G,Std,Pst	
J0617+2238	189.00	+3.05	0.25	0.10	0.46	0.82	12	U0,SNR,RSN,Std,Pst	IC 443
J0622-1139	220.16	-11.69	1.04	0.26	1.96	1.08	5	QSO	0616-116
J0631+0642	204.71	-1.30	0.01	0	1.16	...	13	U0,RSN,Std	
J0633+1751	195.13	+4.27	0.10	0.06	0.16	...	10	PSR	Geminga
J0634+0521	206.18	-1.41	0.01	0	1.12	...	13	U0,Of,OB,Std	
J0702-6212	272.65	-22.56	1.01	0.34	1.65	1.06	9	U15,Std	
J0706-3837	249.57	-13.76	0	0	1.75	...	4	U5,G	
J0721+7120	143.98	+28.02	0	0	0.41	...	5	BLL	0716+714
J0724-4713	259.00	-14.38	1.16	0.57	1.94	2.02	6	U5,G,Std	
J0725-5140	263.29	-16.02	0.89	0.29	1.64	1.18	7	U15,G,Std,Pst	
J0737+1721	201.85	+18.07	0	0	0.70	...	3	BLL	0735+178
J0743+5447	162.99	+29.19	1.21	0.67	2.06	4.78	5	QSO	0738+5451
J0747-3412	249.35	-4.48	0.59	0	1.55	0.29	6	U0,WR,G,Std	
J0808+4844	170.46	+32.48	0	0	0.65	...	5	a	0804+499?, 0809+483?
J0808+5114	167.51	+32.66	0	0	1.18	...	4	a	0803+5126
J0808-5344	268.24	-11.20	1.04	0.55	1.68	2.16	8	U5,G,Std	
J0812-0646	228.64	+14.62	0	0	0.90	...	2	a	0805-077
J0821-5814	273.10	-12.04	1.16	0.46	1.84	1.05	8	U5,G	
J0828+0508	219.60	+23.82	0	0	2.17	...	2	BLL	0829+046
J0834-4511	263.55	-2.79	0.16	0.10	0.28	0.61	7	PSR	Vela

TABLE 1. VARIABILITY  $\delta$  OF SOURCES IN THE THIRD EGRET CATALOG— *Continued*

3EG Name	$\ell$ (deg)	b (deg)	$\delta$	$\delta_{\min}$	$\delta_{\max}$	$V_{12}$	Num Obs	Classes	ID
J0845+7049	143.54	+34.43	0.62	0.23	1.43	1.38	4	QSO	0836+710
J0852-1216	239.06	+19.99	1.21	0.52	2.26	1.94	4	QSO	PMN J0850-1213
J0853+1941	206.81	+35.82	0	0	0.81	...	3	BLL	0851+202
J0903-3531	259.40	+7.40	0.52	0	1.28	0.70	7	U5,Std	
J0910+6556	148.30	+38.56	0.64	0	1.61	0.60	4	U30,Std	
J0917+4427	176.11	+44.19	0	0	0.53	...	5	a	0917+449
J0952+5501	159.55	+47.33	0.39	0	0.88	0.31	9	QSO	0954+556
J0958+6533	145.75	+43.13	0.96	0.42	1.72	2.29	6	BLL	0954+658
J1009+4855	166.87	+51.99	0	0	0.94	...	9	a	1011+496
J1013-5915	283.93	-2.34	0.14	0	0.52	0.18	9	U0,G,RSN,Std,Pst,PWN	
J1014-5705	282.80	-0.51	0	0	0.55	...	10	U0,G,Std,Pst,noPWN	
J1027-5817	284.94	-0.52	0.21	0	0.46	0.39	9	U0,OB,G,Std,Pst	
J1045-7630	295.66	-15.45	0	0	0.44	...	7	U15,Std,Pst	
J1048-5840	287.53	+0.47	0	0	0.31	...	8	PSR,Std	PSR B1046-58
J1052+5718	149.47	+53.27	0.24	0	1.02	0.10	6	a	1055+567
J1058-5234	285.98	+6.65	0	0	0.47	...	8	PSR	PSR B1055-52
J1102-6103	290.12	-0.92	0	0	1.08	...	7	U0,WR,OB,G,SNR,Std,Pst,noPWN	MSH 11-62
J1104+3809	179.83	+65.03	0.35	0	0.80	0.46	7	BLL	Mrk 421
J1133+0033	264.52	+57.48	0.82	0	1.51	0.65	8	U30	
J1134-1530	277.04	+43.48	1.12	0.61	1.84	3.79	7	a	1127-145
J1200+2847	199.42	+78.38	1.17	0.75	1.77	5.49	9	QSO	1156+295
J1212+2304	235.57	+80.32	0	0	1.13	...	11	U30	
J1219-1520	291.56	+46.82	1.10	0.56	1.72	1.77	9	U30	
J1222+2315	241.87	+82.39	1.09	0.60	1.65	1.61	10	U30	
J1222+2841	197.27	+83.52	0.62	0.22	1.20	1.17	8	BLL	1219+285
J1224+2118	255.07	+81.66	0.45	0	0.98	0.62	9	QSO	1222+216
J1227+4302	138.63	+73.33	1.36	0.76	2.37	2.34	4	U30	
J1229+0210	289.95	+64.36	0.46	0.22	0.85	1.56	8	QSO	3C 273
J1230-0247	292.58	+59.66	0.59	0	1.31	0.71	8	QSO	1229-021
J1234-1318	296.43	+49.34	0.61	0	1.33	0.77	8	U30,Std,Pst	
J1235+0233	293.28	+65.13	0.21	0	0.86	0.11	8	U30,Std,Pst	
J1236+0457	292.59	+67.52	0.53	0	1.42	0.10	8	a	1237+0459
J1246-0651	300.96	+55.99	0.60	0.11	1.23	0.89	8	QSO	1243-072
J1249-8330	302.86	-20.63	0.71	0	1.64	0.62	6	U15,Std	
J1255-0549	305.09	+57.06	0.90	0.65	1.35	$\infty$	8	QSO	3C 279
J1300-4406	304.60	+18.74	0.54	0	1.40	0.30	8	U15,Std	
J1308+8744	122.74	+29.38	0	0	0.94	...	6	U15,Std	
J1308-6112	305.01	+1.59	0.72	0.29	1.45	1.37	8	U0,OB,G,Std	
J1314-3431	308.21	+28.12	0	0	0.42	...	6	a	1313-333
J1316-5244	306.85	+9.93	0.42	0	0.98	0.49	8	U5,G,Std,Pst	
J1323+2200	359.33	+81.15	1.09	0.52	1.79	1.61	7	a	1324+224
J1324-4314	309.32	+19.21	0	0	0.49	...	8		Cen A
J1329+1708	346.29	+76.68	0.62	0	1.36	0.14	9	QSO	1331+170
J1329-4602	309.83	+16.32	0	0	0.76	...	8	U15,Std,Pst	
J1337+5029	105.40	+65.04	0.53	0	1.30	0.41	5	U30,Std,Pst	
J1339-1419	320.07	+46.95	0.81	0	1.56	0.34	7	QSO	1334-127
J1347+2932	47.32	+77.50	0.64	0	1.60	0.40	6	U30,Std	
J1409-0745	333.88	+50.28	1.42	1.00	2.07	$\infty$	8	QSO	1406-076
J1410-6147	312.18	-0.35	0.32	0.08	0.64	0.76	8	U0,Of,OB,G,SNR,RSN,Std,Pst,noPWN	G312.4-0.4
J1420-6038	313.63	+0.37	1.03	0.37	1.83	1.59	8	U0,OB,G,Std,Pst,PWN	
J1429-4217	321.45	+17.27	0.93	0.44	1.58	2.15	9	QSO	1424-418
J1447-3936	326.12	+17.96	0.28	0	1.07	0.09	9	U15,G,Std,Pst	
J1457-1903	339.88	+34.60	0.49	0	1.65	0.07	6	U30,Std	
J1500-3509	330.91	+20.45	0	0	0.92	...	9	U15,G,Std,Pst	
J1504-1537	344.04	+36.38	1.24	0.58	2.15	1.79	5	a	1504-166
J1512-0849	351.49	+40.37	0	0	0.52	...	5	QSO	1510-089
J1517-2538	339.76	+26.60	0	0	1.59	...	6	a	1514-241
J1527-2358	342.97	+26.50	0.92	0	1.71	0.07	9	U15	
J1600-0351	6.30	+34.81	0.01	0	1.62	...	4	U30	
J1605+1553	29.18	+43.84	0	0	0.70	...	2	BLL	1604+159
J1607-1101	0.91	+29.05	1.45	0.93	2.10	0.93	10	U15	
J1608+1055	23.03	+40.79	1.09	0.25	2.72	1.15	2	QSO	1606+106
J1612-2618	349.76	+17.64	1.04	0.48	1.62	1.47	12	U15,G	
J1614+3424	55.15	+46.38	0	0	0.41	...	2	QSO	1611+343
J1616-2221	353.00	+20.03	0	0	0.54	...	12	U15,G,Std,Pst	
J1621+8203	115.53	+31.77	0	0	0.52	...	4	U30,Std	
J1625-2955	348.82	+13.32	1.62	1.22	2.19	$\infty$	12	QSO	1622-297
J1626-2519	352.14	+16.32	1.05	0.54	1.60	2.03	13	QSO	1622-253
J1627-2419	353.36	+16.71	0	0	0.57	...	12	U15,G,Std,Pst	
J1631-1018	5.55	+24.94	0.35	0	1.01	0.21	12	U15,G,Std,Pst	
J1631-4033	341.61	+5.24	0.31	0	0.90	0.16	14	U5,G,Std	
J1633-3216	348.10	+10.48	0.59	0	1.25	0.50	13	U5,G,Std	
J1634-1434	2.33	+21.78	0	0	0.88	...	12	U15,G,Std,Pst	
J1635+3813	61.09	+42.34	0	0	0.55	...	2	QSO	1633+382
J1635-1751	359.72	+19.56	0.83	0	1.48	0.16	13	U15,G	
J1638-2749	352.25	+12.59	0.47	0.17	0.88	1.06	14	U5,G,Std,Pst	

TABLE 1. VARIABILITY  $\delta$  OF SOURCES IN THE THIRD *EGRET* CATALOG— *Continued*

3EG Name	$\ell$ (deg)	b (deg)	$\delta$	$\delta_{\min}$	$\delta_{\max}$	$V_{12}$	Num Obs	Classes	ID
J1638–5155	334.05	–3.34	0.19	0	0.91	0.13	13	U0,Std,Pst	
J1639–4702	337.75	–0.15	0	0	0.57	...	12	U0,OB,RSN,Std,Pst,noPWN	
J1646–0704	10.85	+23.69	0.75	0	1.41	0.76	12	U15,G,Std,Pst	
J1649–1611	3.35	+17.80	0	0	1.21	...	14	U15,G,Std,Pst	
J1652–0223	15.99	+25.05	0	0	0.96	...	6	U15,G,Std,Pst	
J1653–2133	359.49	+13.81	0.95	0	1.51	0.73	14	U5,G	
J1655–4554	340.48	–1.61	0.78	0.18	1.50	0.97	13	U0,WR,OB,Std,Pst	
J1659–6251	327.32	–12.47	0.73	0	1.66	0.47	6	U5,Std	
J1704–4732	340.10	–3.79	1.37	0.91	1.93	2.67	13	U0	
J1709–0828	12.86	+18.25	0.67	0	1.40	0.37	11	U15,G,Std,Pst	
J1710–4439	343.10	–2.69	0.07	0	0.21	...	14	PSR	PSR B1706–44
J1714–3857	348.04	–0.09	0.17	0	0.52	0.29	13	U0,RSN,Std,Pst,noPWN	
J1717–2737	357.67	+5.95	0.91	0.50	1.43	2.72	15	U5,Std,Pst	
J1718–3313	353.20	+2.56	0.82	0.43	1.36	2.50	15	U0,OB	
J1719–0430	17.80	+18.17	0	0	0.81	...	8	U15,G,Std,Pst	
J1720–7820	314.56	–22.17	0.64	0	2.13	0.02	3	a	1716–771
J1726–0807	15.52	+14.77	0.45	0	1.03	0.36	12	U5,G,Std,Pst	
J1727+0429	27.27	+20.62	0	0	0.74	...	3	QSO	1725+044
J1733+6017	89.12	+32.94	0.29	0	1.32	0.15	4	U30,Std	
J1733–1313	12.03	+10.81	0.37	0.14	0.68	1.01	12	QSO	1730–130
J1734–3232	355.64	+0.15	0	0	0.37	...	16	U0,OB,RSN,Std,Pst	
J1735–1500	10.73	+9.22	0.87	0	1.45	0.38	14	U5,G	
J1736–2908	358.79	+1.56	0.64	0.31	1.12	1.67	15	U0,Std,Pst	
J1738+5203	79.37	+32.05	0.51	0.10	1.37	0.85	3	QSO	1739+522
J1741–2050	6.44	+5.00	0	0	0.57	...	14	U5,Std,Pst	
J1741–2312	4.42	+3.76	0.26	0	0.78	0.15	14	U0,Std,Pst	
J1744–0310	22.19	+13.42	0.59	0	1.49	0.52	7	QSO	1741–038
J1744–3011	358.85	–0.52	0.30	0	0.61	0.64	15	U0,RSN,Std,Pst	
J1744–3934	350.81	–5.38	0.60	0.04	1.14	0.82	12	U5,Std,Pst	
J1746–1001	16.34	+9.64	0.42	0	0.88	0.54	12	U5,G,Std,Pst	
J1746–2851 <sup>a</sup>	0.11	–0.04	0.48	0.29	0.75	2.35	15	U0,RSN,Std,Pst	
J1757–0711	20.30	+8.47	0.51	0	1.11	0.42	14	U5,G,Std,Pst	
J1800–0146	25.49	+10.39	0	0	0.58	...	8	U5,G,Std,Pst	
J1800–2338	6.25	–0.18	0.16	0	0.58	0.26	16	U0,SNR,RSN,Std,Pst	W28
J1800–3955	352.45	–8.43	0	0	1.13	...	13	QSO	1759–396
J1806–5005	343.29	–13.76	0.88	0	1.56	0.34	10	a	PMN J1808–5011
J1809–2328	7.47	–1.99	0.71	0.46	1.13	3.93	15	U0,OB,Std,Pst	
J1810–1032	18.81	+4.23	0	0	0.58	...	14	U0,Std	
J1812–1316	16.70	+2.39	0.82	0.47	1.35	2.73	15	U0,Std,Pst	
J1813–6419	330.04	–20.32	0	0	0.97	...	4	U15,Std,Pst	
J1822+1641	44.84	+13.84	1.11	0.54	2.10	2.26	4	U5,G	
J1823–1314	17.94	+0.14	0.60	0.21	1.18	1.18	14	U0,OB,SNR,Pst	Kes 67
J1824+3441	62.49	+20.14	0.01	0	1.30	...	8	U15,G	
J1824–1514	16.37	–1.16	0	0	0.84	...	14	U0,OB,RSN,Std,Pst,noPWN	
J1825+2854	56.79	+18.03	0	0	1.33	...	7	U15,G	
J1825–7926	314.56	–25.44	0.76	0	1.77	0.78	4	U15,Std,Pst	
J1826–1302	18.47	–0.44	0.88	0.50	1.45	3.22	14	U0,OB,Std,Pst	
J1828+0142	31.90	+5.78	1.60	1.02	2.48	6.89	6	U5	
J1832–2110	12.17	–5.71	0.62	0.19	1.20	1.05	13	QSO	1830–210
J1834–2803	5.92	–8.97	0	0	0.59	...	14	U5,Std,Pst	
J1835+5918	88.74	+25.07	0.15	0	0.47	0.09	4	U15,Std,Pst,Gem	
J1836–4933	345.93	–18.26	0	0	0.97	...	9	U15,Std,Pst	
J1837–0423	27.44	+1.06	1.50	0.97	2.26	2.95	8	U0,RSN,PWN	
J1837–0606	25.86	+0.40	0	0	0.67	...	8	U0,Std,Pst,noPWN	
J1847–3219	3.21	–13.37	0.75	0	1.36	0.71	14	U5,Std	
J1850+5903	88.92	+23.18	0	0	1.58	...	5	U15	
J1850–2652	8.73	–11.76	0.81	0	1.42	0.59	13	U5	
J1856+0114	34.60	–0.54	0.71	0.28	1.53	1.57	6	U0,SNR,RSN,Std,Pst,PWN	W44
J1858–2137	14.21	–11.15	0	0	0.80	...	12	U5,Std,Pst	
J1903+0550	39.52	–0.05	0	0	0.42	...	5	U0,SNR,RSN,Std,Pst	G40.5–0.5
J1904–1124	24.22	–8.12	0.08	0	0.76	...	10	U5,Std,Pst	
J1911–2000	16.87	–13.22	0.30	0	0.82	0.25	11	QSO	1908–201
J1921–2015	17.81	–15.60	1.24	0.80	1.76	2.19	12	a	1920–211
J1928+1733	52.71	+0.07	0.76	0.33	1.57	1.83	6	U0	
J1935–4022	358.65	–25.23	1.34	0.83	2.12	4.41	6	QSO	1933–400
J1937–1529	23.95	–17.12	1.35	0.72	2.05	1.08	8	QSO	1936–155
J1940–0121	37.41	–11.62	1.28	0.70	2.10	2.48	6	U5	
J1949–3456	5.25	–26.29	1.17	0.64	1.84	2.59	8	U15	
J1955–1414	27.01	–20.56	0.84	0.10	1.62	0.88	7	U15,Std	
J1958+2909	66.23	–0.16	0.32	0	0.86	0.31	9	U0,Std,Pst	
J1958–4443	354.85	–30.13	0	0	1.64	...	4	U30	
J1959+6342	96.61	+17.10	0	0	0.76	...	6	U15,Std,Pst	
J2006–2321	18.82	–26.26	1.31	0.73	2.12	2.63	6	U15	
J2016+3657	74.76	+0.98	0.44	0	1.02	0.63	9	U0,WR,OB,RSN,Std,Pst	
J2020+4017	78.05	+2.08	0.06	0	0.24	...	9	U0,OB,G,SNR,RSN,Std,Pst,Gem	$\gamma$ Cyg
J2020–1545	28.09	–26.62	0	0	1.30	...	4	U15,Std	

TABLE 1. VARIABILITY  $\delta$  OF SOURCES IN THE THIRD EGRET CATALOG— *Continued*

3EG Name	$\ell$ (deg)	b (deg)	$\delta$	$\delta_{\min}$	$\delta_{\max}$	$V_{12}$	Num Obs	Classes	ID
J2021+3716	75.58	+0.33	0.36	0.03	0.83	0.71	9	U0,WR,OB,Std,Pst,PWN	
J2022+4317	80.63	+3.62	0.16	0	0.80	0.12	9	U0,WR,OB,G,Std	
J2025-0744	36.90	-24.38	0.87	0.42	1.81	3.14	4	QSO	2022-077
J2027+3429	74.08	-2.36	0	0	0.43	...	9	U0,OB,Std,Pst	
J2033+4118	80.27	+0.73	0.21	0	0.52	0.40	9	U0,Of,OB,G,Std,Pst	
J2034-3110	12.25	-34.64	1.18	0.55	2.05	1.43	5	U30	
J2035+4441	83.17	+2.50	0.05	0	0.66	...	9	U0,G,Std,Pst	
J2036+1132	56.12	-17.18	0	0	1.30	...	5	BLL	2032+107
J2046+0933	55.75	-20.23	0	0	0.80	...	6	U15,Std	
J2055-4716	352.56	-40.20	0.93	0.34	2.09	1.59	3	QSO	2052-474
J2100+6012	97.76	+9.16	0.13	0	0.70	0.03	6	a	2105+598
J2158-3023	17.73	-52.25	0.59	0	1.66	0.75	3	BLL	2155-304
J2202+4217	92.59	-10.44	0.80	0.02	1.57	0.85	8	BLL	BL Lac
J2206+6602	107.23	+8.34	0	0	0.49	...	5	a	2206+650
J2209+2401	81.83	-25.65	0.91	0	1.86	0.36	5	QSO	2209+236
J2219-7941	310.64	-35.06	0	0	0.89	...	4	U30,Std,Pst	
J2227+6122	106.53	+3.18	0.20	0	0.82	0.21	5	U0,OB,G,Std,Pst,PWN	
J2232+1147	77.44	-38.58	0.48	0.18	0.97	1.22	7	QSO	2230+114
J2241-6736	319.81	-45.02	0	0	1.54	...	3	U30	
J2243+1509	82.69	-37.49	1.06	0	1.79	0.86	7	U30	
J2248+1745	86.00	-36.17	0.65	0	1.48	0.54	7	U30,Std,Pst	
J2251-1341	52.48	-58.91	1.30	0.73	2.19	4.04	5	U30	
J2254+1601	86.11	-38.18	0.52	0.31	0.91	3.93	7	QSO	2251+158
J2255+1943	89.03	-35.43	1.18	0.25	1.95	0.95	7	a	2250+1926
J2255-5012	338.75	-58.12	0.50	0	2.00	0.33	2	U30	
J2314+4426	105.32	-15.10	1.11	0.20	2.39	0.93	3	U15,Std	
J2321-0328	76.82	-58.07	1.36	0.78	2.27	2.46	5	QSO	2320-035
J2352+3752	110.26	-23.54	1.37	0.72	2.43	2.23	4	a	2346+385
J2358+4604	113.39	-15.82	0	0	0.61	...	3	QSO	2351+456
J2359+2041	107.01	-40.58	0.74	0	1.57	0.53	7	QSO	2356+196

NOTE. — The sources marked “a” in the Classes column are low-confidence AGN identifications in the 3EG catalog. For the other Classes, see Table 2.

<sup>a</sup> See text for comments about the variability of 3EG J1746-2851.